



Design and Development of Controlled Docking Mechanism Using Electromagnets for 3U CubeSat

Team Design Project - Group 1
Lehrstuhl für Informatik VIII

Elisa Boccolari Oscar Boo Fernandez Pawan Kumar
Milan Pathak Recep Suluker

11 April 2023

Contents

1	Introduction	4
2	Hardware Modules	5
2.1	STM32F4 Discovery Board	5
2.2	Time-of-Flight Sensors	5
2.3	Raspberry Pi Zero 2W	5
2.4	Motor Driver	5
3	Mechanical Design and Manufacturing	6
3.1	Design	6
3.2	Manufacturing and Assembly	6
3.3	Electromagnets	7
4	Electrical Design	8
4.1	Electrical Design	8
4.2	Electrical Schematics	9
5	Embedded Software	11
5.1	Thread Structure	11
5.2	Middleware	11
5.3	Ranging Thread	11
5.3.1	Median Filter	11
5.4	Telecommand Thread	12
5.5	Electromagnet Thread	12
5.6	Control Thread	12
6	Ground Station	13
6.1	Implementation	13
6.1.1	Front-end	13
6.1.2	Back-end	14
7	Control Design	16
7.1	Magnetic Field Lines Modelling	16
7.2	Control Modes	17
7.2.1	Distance-based Control	18
7.2.2	Velocity-and-Distance-based Control	18
7.2.3	Orientation Control	19
8	Testing Environment	21
8.1	Testing Conditions	21
8.2	Test Platforms	21
8.2.1	Hanging the satellites from the ceiling	21
8.2.2	Hanging the satellites from sliders	21
8.2.3	Mounting the satellites in friction-less vehicles	22
8.3	Conducting the tests	23
8.3.1	Study of the maximum distance for operations	23

8.3.2	Study of the maximum angle for operations	23
8.3.3	Study of the capability of Undocking	24
8.3.4	Study of the interaction with Earth’s magnetic field	24
8.3.5	Study of the maximum temperature of the mockups	24
8.3.6	Distance control tests	24
8.3.7	Velocity control tests	25
9	Results	26
9.1	Test Results on Multiple Platforms	26
9.2	Physical Constraints	27
9.2.1	Effect of different structure surface on controller	27
9.2.2	Polarity of the electromagnets	27
9.2.3	Heat generation	29
9.3	Undocking	29
9.4	Interaction with Earth’s magnetic field	30
9.5	Power Constraints	30
9.6	Control Constraints	30
10	Recommendations and Future Work	32
11	Conclusion	33

1 Introduction

TAMARIW stands for TeilAutonome Montage/Aufbau und Rekonfiguration Im Weltraum, which means Semi-autonomous Assembly/Construction and Reconfiguration in Space. The primary goal of the project is to demonstrate if two 3U CubeSats equipped with 4 electromagnets each, have the ability to perform docking and undocking maneuvers in space taking advantage of electromagnetic force.

Both satellites are developed simultaneously and they are exact replicas. Their structures are designed to have one of their main faces ($300 \times 100\text{mm}$) as the docking side. The docking side has four electromagnets placed at the corners in order to ease the alignment of the satellites as they will be driven through H-bridge and controlled via PWM. This allows controlling the polarity of the electromagnets and their strength.

To properly control the satellites, other sensors are included on the docking side: 4 Time-of-Flight proximity sensors (Lidar) to identify the distance and velocity from each other, and a minimum of 8 LEDs and a camera to identify the docking surface and the orientation.

As this is a complex project that includes several tasks, it was divided into 3 different teams that would focus on different aspects. The objectives that our group aimed to achieve are:

- Definition of the mechanical and electrical design of a 3U CubeSat mock-up that includes all the necessary components (sensors, microcontroller, Lidars, etc.).
- Building of two functional mock-ups.
- Implementation of a relative distance and orientation system using the Lidars.
- Implementation of a simple controller for the electromagnetic force, where feedback from proximity sensors will be used to indicate the relative velocity and orientation of the other satellite.
- Testing: Definition of the operational workspace.

The start point of this project was a similar project conducted by other colleagues, who tried to achieve the goal using permanent magnets, and found out that the docking was not safe using these magnets. Moreover, their results helped to have a rough estimation of the mass, and the electronic components needed, or to establish the number of Lidars.

2 Hardware Modules

In order to realize and test the design, multiple hardware modules were utilized including the feedback sensors, a microcontroller, and actuators. This section elaborates on the hardware modules used in this project.

2.1 STM32F4 Discovery Board

For the microcontroller, STM electronics STM32F4 discovery board was used as a primary onboard processing unit [1]. Its $16MHz$ oscillator with ARM CORTEX-M4 MCU alongside the dedicated input/output pins meets all the requirements needed for this project.

2.2 Time-of-Flight Sensors

The lidar-based ToF sensors are the core sensors of the design to get the relative distance between two satellites, which is consequentially used to calculate the relative velocity. In this project, ST electronics VL53L4CD ToF sensors [5] were used and each mockup was equipped with four of those sensors. These sensors are specifically designed to serve short-range measurements with low power consumption, which makes them an optimal choice for the purpose. In addition, equipping four of them on a single mock-up ensure that even in slight disturbance, a relatively accurate value of relative distance can be obtained. These sensors use an I^2C interface for the transfer of data, alongside the GPIO pins to call for the interrupt.

2.3 Raspberry Pi Zero 2W

Integration of Raspberry Pi Zero 2W [4] in the mockups was another requirement for the project. Although using it for computations was out of the scope of this project nonetheless, ground-station connectivity with STM32 discovery was established by using Raspberry Pi's built-in wireless connectivity feature. Hence its sole purpose was to make wireless connectivity feasible.

2.4 Motor Driver

To operate and control the current flowing through the electromagnets, a single channel H-bridge DC motor driver namely Toshiba's TB9051FTG [3] was used. This motor board operates between $4.5V$ and $28V$ and can give $5A$ maximum current with current limitation control. In these mockups, each electromagnet is connected and controlled by one of such drivers. By using the PWM signal pins, both reverse and forward current modes are utilized. In addition, the onboard OCM pin provides voltage-based current feedback sense which is used to compute the current ratings of electromagnets. For further details on electrical pin schematics, refer to Section 4.2.

3 Mechanical Design and Manufacturing

3.1 Design

The mechanical structure had to be designed and manufactured within the specified limit of $340.5\text{mm} \times 108\text{mm} \times 108\text{mm}$. This dimension was referenced from the CAD model of TAMARIW which was provided. Two identical 3U CubeSats were designed where one side of the satellite is a docking side consisting of four electromagnets placed at the corner which will help in the alignment of the satellites by controlling the magnetic force via PWM signals.

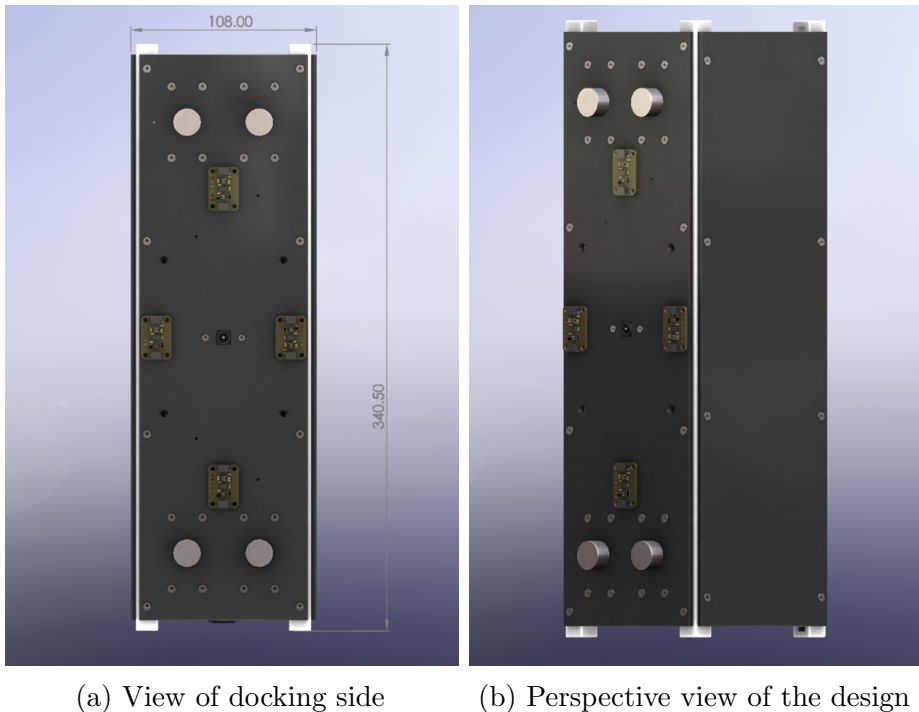
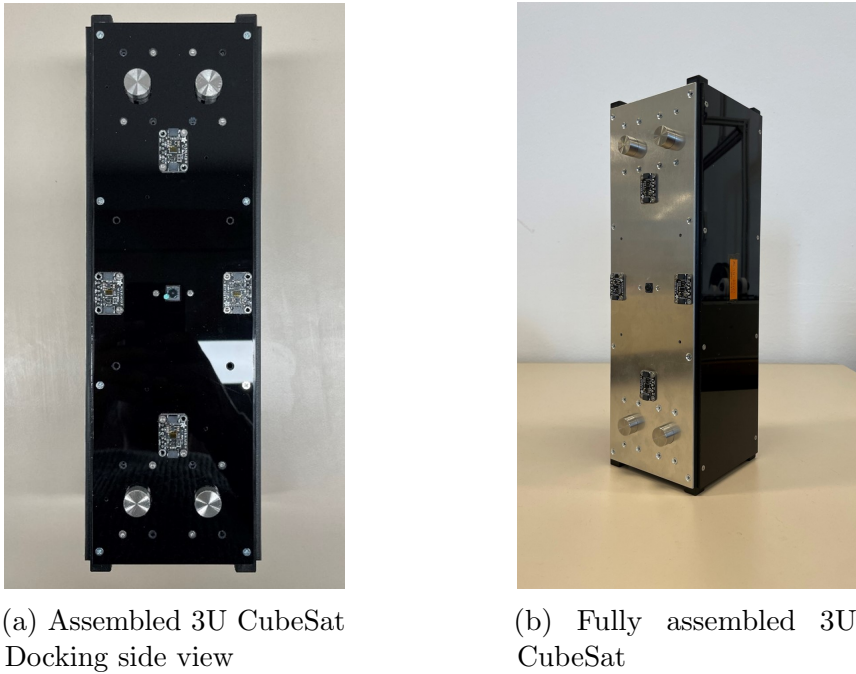


Figure 1: Complete Design of 3U Cubesat

As shown in Figure 1, the dimensions of the 3U CubeSat are $340.5 \times 108 \times 108$ mm. The design was done in Solidworks 2021. The materials for each component were assigned in Solidworks and for those whose actual mass was not available, the components were measured individually and their masses were updated in the design. As per the design, the calculated mass of each satellite is 2500g.

3.2 Manufacturing and Assembly

The mockups were manufactured using Plexiglass and PLA (polylactic acid). The main supporting rails were 3D printed using PLA and the panels were made from 3mm plexiglass by laser cutting. The docking panel was later replaced by a 2mm aluminum panel to improve lidar accuracy. The mechanical structure includes ports for charging, and debugging, a power switch, and UART at the top. Figure 2 shows a completed 3U CubeSat model. Figure 2b shows the docking side with the aluminum plate replacement. The mass of each satellite after complete assembly is 2533.75g.



(a) Assembled 3U CubeSat
Docking side view

(b) Fully assembled 3U
CubeSat

Figure 2: Completed Assembly of 3U CubeSat

3.3 Electromagnets

The core of the electromagnet is made from a nickel-iron alloy called Invar36. The underlying idea behind using this type of core was its dimensional stability over a wide range of temperatures, making it a suitable candidate for the task it was designated for. The copper wire with a diameter of $0.75mm$ was wounded on the core with a number of turns that varies between 530 and 560 using a winding machine. The casing for the electromagnets was 3D printed using PLA. These electromagnets were designed to operate at the current of $2A$ at $5V$ to generate a maximum magnetic field strength of $70mT$ at the surface of the core. This strength was controlled by setting different duty-cycle commands. In Table 1 the specifications for the electromagnets are listed.

Parameter	Value
Core diameter	$16mm$
Core length	$60.1mm$
Total diameter	$32mm$
N° of turns	550
Total length of the wire	$33m$
Diameter of the wire	$0.75mm$
Mass of the Electromagnet	$240g$
Max. current	$2A$
Max. voltage	$5V$
Max. power	$10W$

Table 1: Electromagnets Specification

4 Electrical Design

4.1 Electrical Design

The internal components of the Electrical Subsystem consist of Raspberry Pi for Image processing, STM32F4 Discovery board for Lidar distance measurements and TB9051FTG motor driver for PWM control of Electromagnets. The system is powered using two LiFe batteries (6.6V, 2100mAh) connected in parallel.

As depicted in Figure 3 the electrical subsystem is stacked on top of each other to create a single module where all the wires can be plugged in. The subsystem also includes connections for the power system, with a relay to switch high current. The maximum current flowing through the system is 9A, 2A for each electromagnet, and 1A for powering lidars, STM32F4 Discovery board, and Raspberry Pi. The electrical system is designed to handle 9A continuous current for half an hour but, at maximum capacity, the batteries are discharged within 15 minutes. So, the design is within the specifications and a safe limit. Figure 4 shows a completed electrical system implemented in the 3U CubeSat with all the necessary wiring and connections.

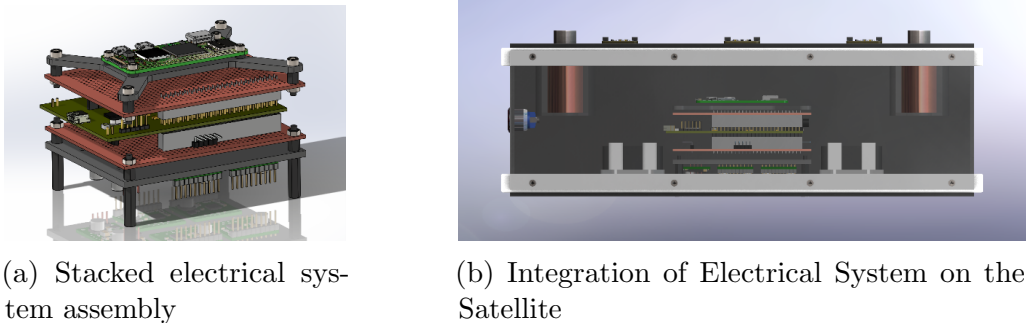


Figure 3: 3D design and integration of Electrical System in the Satellite



Figure 4: Complete Electrical Assembly of 3U Cubesat

4.2 Electrical Schematics

In this section, the schematics of the electrical connections will be presented. Note that for simplicity, the schematics were divided into 2 different files: Figure 5 describes how every component is powered, whereas Figure 6 includes the connections between the Pins of each component and the STM32 controller. This division was useful to understand the electrical components of the project and provided flexibility to do any alterations in the initial design if needed.

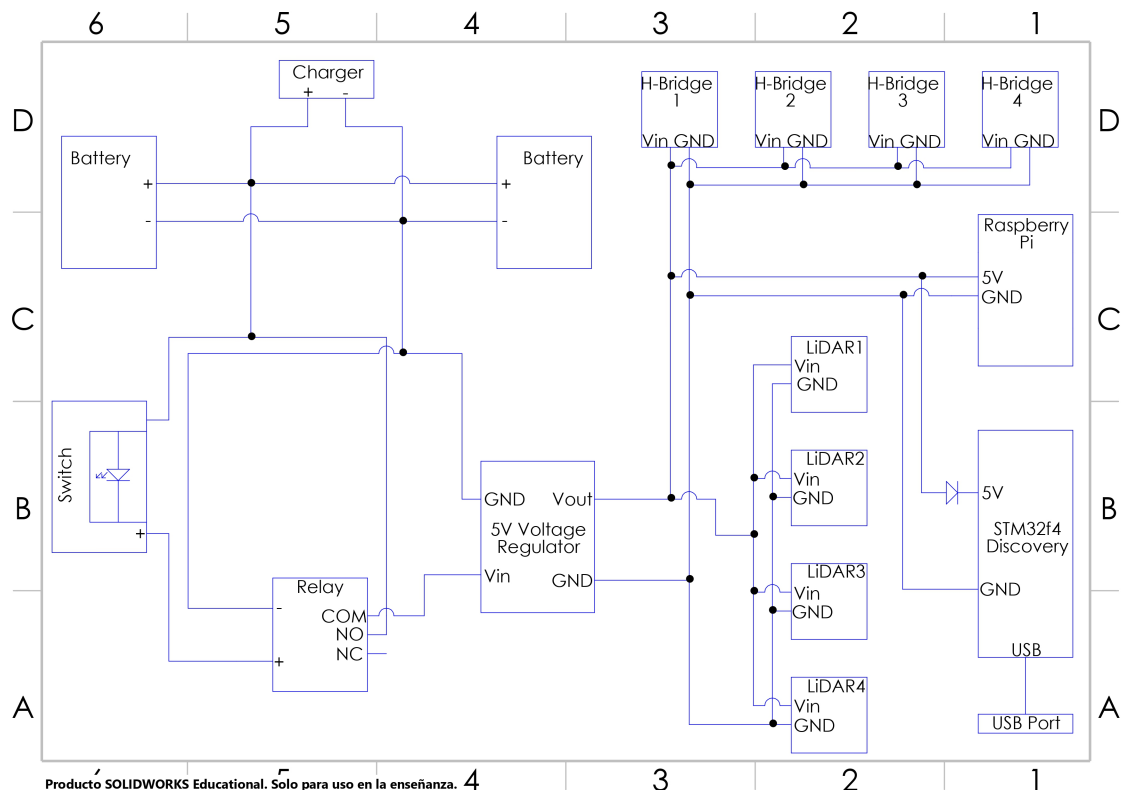


Figure 5: Power schematics

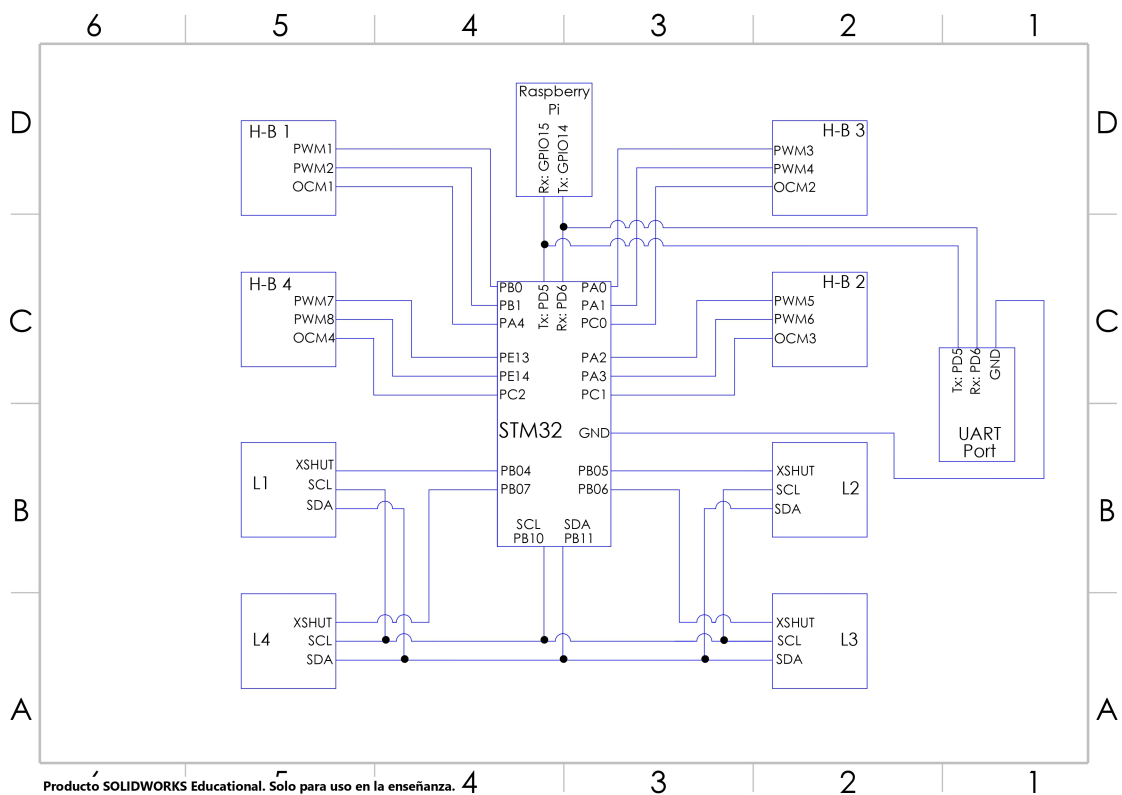


Figure 6: Pins schematics

5 Embedded Software

The main objective of the embedded software is to collect telemetry data from the sensors, transmit them to the ground station and be able to control the CubeSats' attitude both autonomously and with telecommand. The two mock-ups have been programmed using the real-time operating system RODOS with the programming language C++. The complete code can be found in the GitLab repository: https://gitlab.informatik.uni-wuerzburg.de/s426182/tamariv_docking/.

5.1 Thread Structure

Four threads run continuously on the mock-ups, as can be seen in Table 2.

Name	Description	Priority
Ranging	- Calibrates LIDAR sensors - Gets values from LIDAR sensor	100
Telecommand	-Receives and parse telecommands from ground station	100
Electromagnet	- Calculates orientation (pitch and yaw) - Calculates relative velocity - Calculates current to the electromagnets - Sets PWM of electromagnets	100
Control	-Calculates optimal PWM based on the selected mode	100

Table 2: Threads

5.2 Middleware

To share data between the threads the RODOS Middleware has been used. It is an asynchronous way to exchange messages, using the publisher-subscriber protocol.[2]

5.3 Ranging Thread

The main purpose of the ranging thread is to retrieve the values of all the lidar sensors. To do this, it was important to change the default addresses of all the sensors and then initialize them. In addition to that, this thread also calibrates the lidar values and set the offset during the initialization.

5.3.1 Median Filter

To reduce the variation in the values of the sensor, a median filter was implemented that takes the median distance, velocity, and pitch and yaw angles. The median filter takes the N neighbor values of the current one (with N being the size of the filter) and returns the median, filtering out the extreme values due to the low accuracy of the ToF sensors.

5.4 Telecommand Thread

The telecommand thread receives the commands from the ground station, parses them, and then distributes them to the appropriate thread. These telecommands are sent from the web server through WiFi to the Raspberry Pi, which is connected serially (via UART) to the microcontroller, allowing it to control and monitor the satellite remotely. To provide the commands to the other threads, multiple flags are set to switch between the operational behavior of the system.

5.5 Electromagnet Thread

The electromagnet thread is responsible for different tasks. It is a subscriber of the common buffer of the control, telecommand, and ranging threads, which means that it receives and sorts all the information that is then sent to the Raspberry Pi via UART. It includes a function that, based on the lidars' distances, calculates the pitch and yaw angles. Each angle is calculated from the information of two lidars, in the best case the ones with a larger separation along that axis. The thread calculates the mean distance, sorting all the lidars' values from the lowest to the greatest and excluding the minima and the maxima. This was done to try to reduce the error caused by the bad alignment of the satellites. In addition to that, it also contains the current reading function from the OCM pin of the motor driver, which includes initializing the required Analog-to-Digital (ADC) channel and timer to read the analog value and then convert it into a digital value, while also converting the voltage-feedback from this pin to the current. For more details refer to Section 2.4. As a last thing, it sets the PWM of the four electromagnets with the input provided by the control mode or the user's telecommand.

5.6 Control Thread

The main purpose of the control thread is to implement the control algorithm, better described in Section 7. This thread is subscribed to both ranging and electromagnet thread to perform needed calculations for controlling the docking maneuver. The overall thread architecture comprises multiple control functions including orientation control, distance-based and velocity-based controllers that are then implemented together in accordance with the overall control architecture.

6 Ground Station

To establish wireless connectivity with the mockups, a ground station was developed. By doing that, the need for external cables, which could have caused some disturbance forces that can hinder the performance of electromagnets and the air-bearing structure to a certain degree, was eliminated. With this realization, a simple ground station was developed. The idea was to use the WiFi readily available on Raspberry Pi Zero 2W to host a web server on a local network. As Raspberry Pi is quite capable, the idea was implemented and a ground station was developed.

6.1 Implementation

The ground station for the project is a web server hosted by Raspberry Pi zero 2W using a flask module so that the users on the same local network can access the web server, read the data and send commands. The Raspberry Pi executes software algorithms, processes sensor data, and manages communication between the CubeSats and the web-based control panel. The Raspberry Pi 2GB model offers adequate processing power and memory capacity for the complex calculations and real-time data processing required during docking and undocking procedures. There are 14 data points that Raspberry Pi reads from serial, separates them into individual data points, and maps them to a designated field on a table. This is handled by a combination of Python code and an HTML script running continuously on the Raspberry Pi.

6.1.1 Front-end

The front end consists of an HTML (HyperText Markup Language) page where the user can read the data and send commands. The HTML file defines the web page's structure, layout, and content, including the Telemetry Center, Telecommand Center, and Manual PWM section. It also incorporates CSS (Cascading Style Sheets) and JavaScript to enhance the appearance and functionality of the web page, as illustrated in Figure 7.

1. **Telemetry Center:** The Telemetry Center is responsible for receiving and displaying real-time data from both CubeSats. This data includes information about the spacecraft's orientation (pitch and yaw angles), distance measurements from four Lidar sensors (L1, L2, L3, L4), the status of the electromagnets (EM1, EM2, EM3, EM4), as well as other essential parameters such as distance, velocity, and current of each 3U CubeSat. This information is crucial for monitoring the health and performance of the satellite and ensuring that the docking and undocking maneuvers are executed correctly.

2. **Telecommand Center:** The Telecommand Center allows operators to send commands to the CubeSats and control their modes of operation. There are four different modes available on the web page: Idle, Auto-Control, Undock, and Distance Control.

- Idle: In this mode, the CubeSats remain stationary and do not engage in any docking or undocking procedures.

- Auto Control: In Auto Control mode, the CubeSats automatically perform docking and undocking maneuvers based on the velocity-based feedback controller.
- Undock: This mode initiates the undocking procedure, during which the CubeSats separate from each other after completing a docking maneuver.
- Distance Control: In Distance Control, the CubeSats are commanded to approach and dock with each other using the electromagnets and guidance from the Lidar sensors.

3. Manual PWM (Pulse Width Modulation) Section: The Manual PWM section provides operators with the ability to manually control the CubeSats' electromagnets. By adjusting the pulse width modulation of each electromagnet, the operators can fine-tune the forces exerted by the magnets during the docking and undocking procedures. This manual control option can be useful in situations where the automatic algorithms may not be sufficient or when testing new docking strategies.

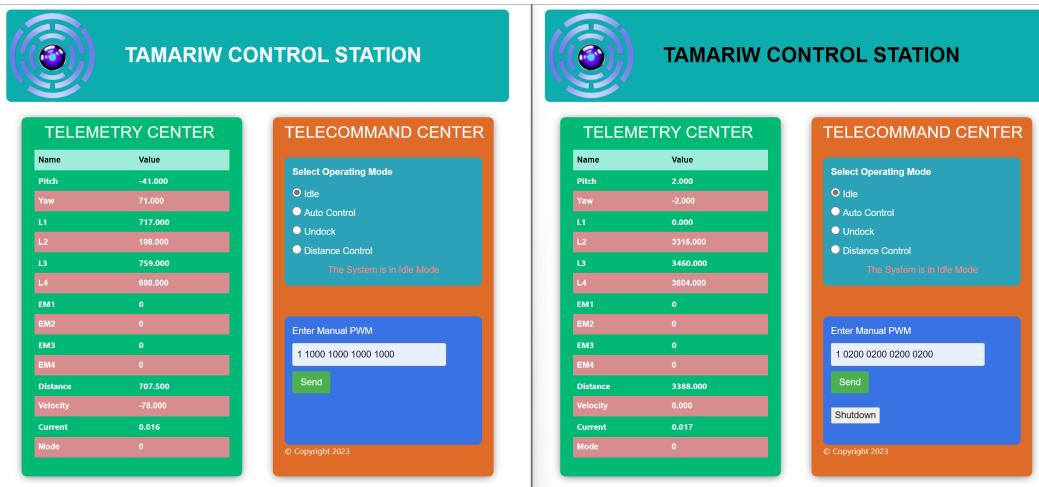


Figure 7: Web Server implemented as a ground station for the satellites

6.1.2 Back-end

The back end is a Python script that uses JavaScript and AJAX to publish and update the data on the web server. Python is chosen for its ease of use, extensive library support, and compatibility with the Raspberry Pi hardware. Instead of refreshing the whole web page, JavaScript listens for any event or change every 300 milliseconds and when there is an update, for example, Lidar value changes, the current information is then updated to that section of the web page only. The implementation of buttons for the operating mode and input field for manual PWM is likewise: they use GET and POST methods to parse the information from the webserver to Raspberry Pi where it writes the information to the microcontroller using UART communication. The web page is deployed on a local web server using the Raspberry Pi hardware, making it

accessible to users on the same local network. The web page can be accessed through two local host addresses: ***192.168.137.208:5000*** and ***192.168.137.85:5000***. These IP addresses correspond to the Raspberry Pi devices hosting the web server, and the port number 5000 indicates the specific network port through which the web page is served.

7 Control Design

For the control part, the main requirement was to perform a docking maneuver between the two satellites in the most controlled way possible. For the scope of this project, only relatively small distances (in the order of 10-30 cm) and pitch/yaw angles were considered, since a thruster-based controller has been developed in parallel by a different team to cope with these types of situations. This turned out to be a more challenging task than expected because it required taking into account many factors and performing numerous tests. The initial idea of devising the control scheme was to use the approach velocity as the controlled parameter and based on that, generate the PWM signal for the electromagnets. Due to this, different control modes were designed and tested on the electromagnets depending on variables such as relative distance, relative orientation, and approach velocity. Given the constraints of magnetic field force and its effect on the subsystems, two different schemes for polarities of electromagnets were tested and their strength as the function of the distance was analyzed, as described in Section 9.2.2. The major obstacle to the implementation of the control system was the sensor values which were not always accurate enough and, in the case of not perfect alignment of the two bodies, completely unreliable.

7.1 Magnetic Field Lines Modelling

The first step in the control design has been defining a simplified analytical model of the behavior of the electromagnets, to determine how the force changes with the increase of the distance and the variation of current. For this purpose, the following equations have been used, which allow us to determine the magnetic force as a function of both relative distance and current and from that, through integration, to calculate the velocity.

$$F = \frac{B^2 A \mu_r}{2 \cdot \mu_0} \quad (1)$$

where F is the electromagnetic force, A is the cross-section area, B is the magnetic field strength, μ_0 is the permeability in free space ($4\pi \cdot 10^{-7}$), μ_r is the relative permeability, which for INVAR 36 is close to the unit and μ is the absolute permeability (product of μ_0 and μ_r).

$$B = \frac{\mu N I}{2 \cdot (r + \frac{d}{2})^2} \quad (2)$$

where B is still the magnetic field strength, μ the absolute permeability, I the current, r the distance between the electromagnets and the target, d the diameter of the target object.

These equations have been used to have a rough idea of the attracting force between the two satellites which is plotted in the Matlab diagram in Figure 8 as a function of the distance and current. It can be seen that at maximum current (2A) and a distance close to 0, the force is about 4.5N for a single electromagnet with the characteristics specified in Table 1 (which has to be multiplied times 8 for all

the electromagnets). The force decreases rapidly due to the inverse square of the distance, reaching $10^{-5} N$ at $15cm$ which is still a relatively high value, especially in LEO orbit, where the higher disturbances are of the order of $10^{-4} N$. Nonetheless, this mathematical model has not been developed further, because it is too far away from the real testing environment. As the matter of fact, it would have been difficult to take into account the combined effect of all the electromagnets, especially with opposite polarity configurations, as shown in Section 9.2.2, or all the disturbances that the testing platforms presented. For these reasons, the development of an empirical model has been favored over an analytical one based on simulations.

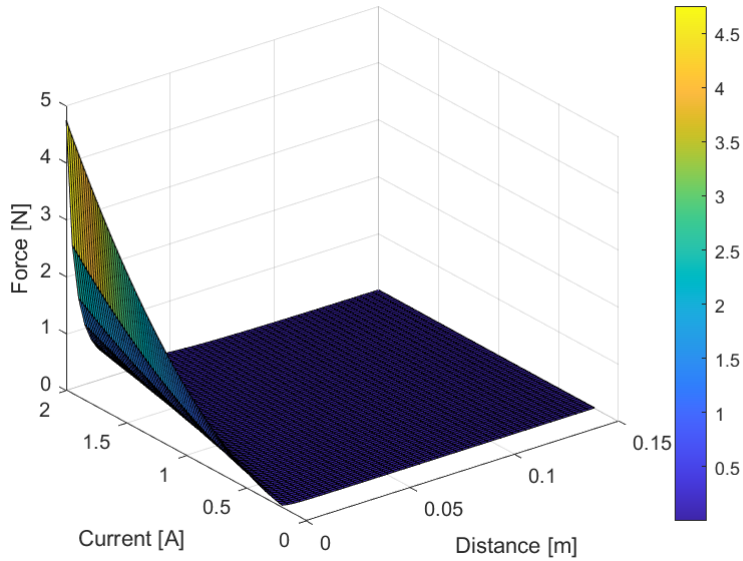


Figure 8: Matlab plot of the variation of Electromagnetic force with distance and current

7.2 Control Modes

The control algorithm has been implemented in RODOS as shown in Figure 9. A series of checks on the relative velocity and position between the two satellites have been implemented to avoid the risk of imperfect docking, which could compromise the whole mission. The risks of a too-fast approach that could cause the crash of the mock-ups in a real-life case and of the approach with the bad alignment that could result in just partial docking (not all the electromagnets of a satellite are in contact with the respective in the other) or a collision with other parts of the satellites, have been taken into account. Once the minimal requirements for a safe dock have been ensured, the real control algorithm was designed to perform the maneuver with a defined velocity. Once the satellites make contact with each other, the controller should be able to keep them docked until the telecommand for undocking has been sent.

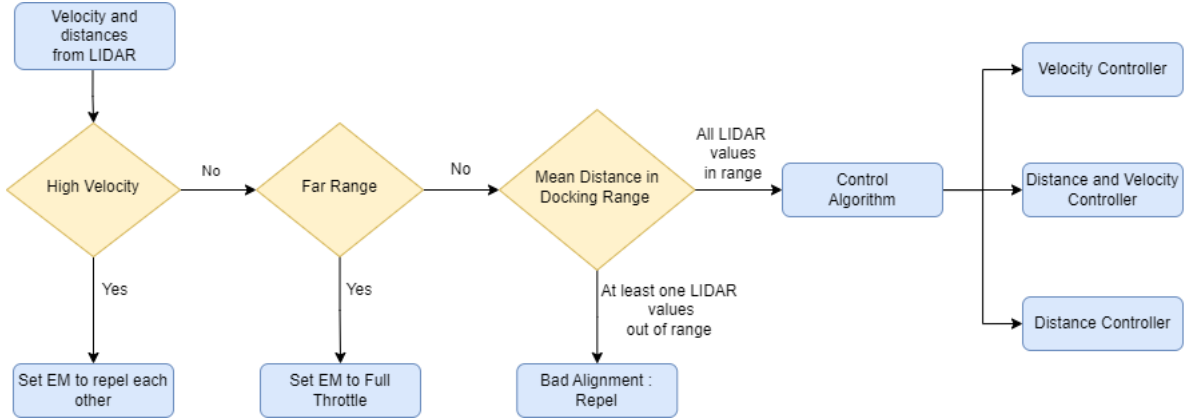


Figure 9: Control Scheme

7.2.1 Distance-based Control

In Figure 10 the flowchart of the control algorithm is displayed. As explained in the preceding section, distance control comes into effect when we reach the docking range, which is found out by performing multiple tests. After coming into this range, the distance controller sets the predefined PWM values to the electromagnets in a manner to ensure a smooth docking maneuver. These predefined PWM values are highly coupled with the test conditions. Nonetheless, the defined distance controller with the combination of general control architecture ensures a smooth approach and docking. It should be noted that those predefined values were chosen to be the same for both satellites hence, it is prone to any disturbances that can give rise to any unwanted motion in satellites. Overall, this controller, in the test environment, yielded good results when satellites were finely orientated toward each other.

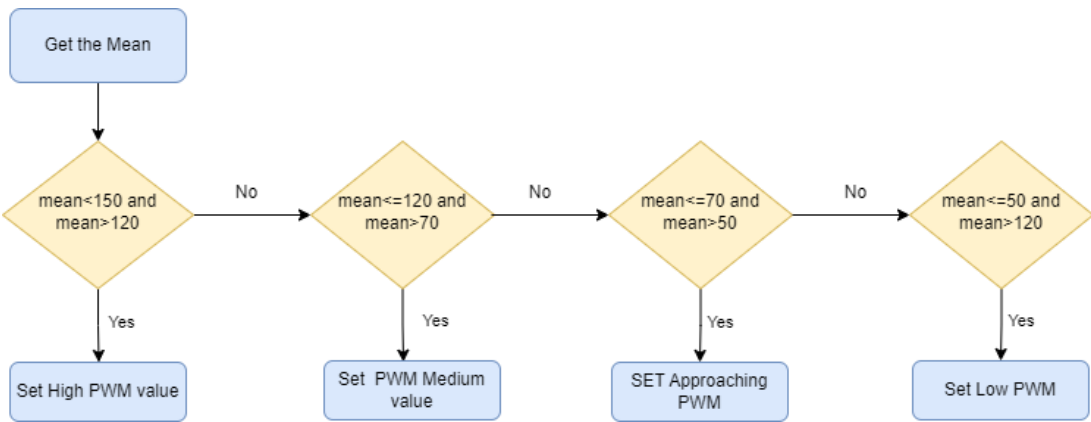


Figure 10: Distance Control Scheme

7.2.2 Velocity-and-Distance-based Control

Even though the distance controller was sufficient to yield results in given test conditions, it did not take any variance in test environments into account. This gave rise to develop an adaptive controller that can perform well when satellites are

introduced to unaccounted disturbances. Therefore, an adaptive velocity controller was designed. This controller relied on both the satellite's approaching velocity and the relative distance as different sets of PID parameters along with distinct target velocities were defined depending upon the relative distance. For instance, during the large mean distance, a higher target velocity was set along with the robust proportional gain value and as the mean distance started decreasing, smaller target velocities were set. By following this approach, it was ensured that the condition of docking meets even when satellites do uncharacteristic behavior during the approach. Tuning multiple PIDs in an empirical system is a complex assignment, especially because the range of action is limited and the controller should be very reactive and have a short settling time. Nonetheless, the implementation of this control architecture into the main control framework ensured that the overall docking operation remained smooth.

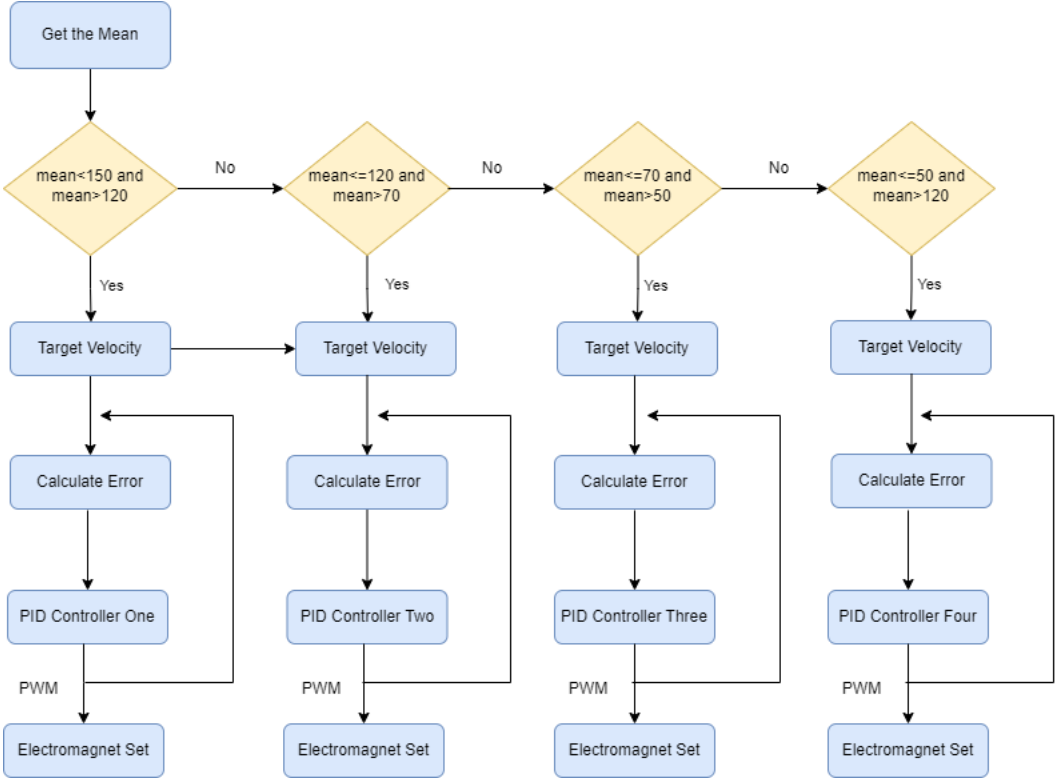


Figure 11: Distance and Velocity Control Scheme

7.2.3 Orientation Control

The additional idea was to check if the orientation of the satellites can be controlled by giving the sequential PWM to the electromagnets to realign themselves. For this purpose, yaw and pitch angles were calculated using the four lidar values, as specified in Section 5.5. It was found that solely relying on the lidar values for controlling the orientation is unconventional and prone to a lot of disturbance as the minimum requirement for getting the orientation angles is to have at least three correct lidar values. A controller was formulated, that functions by powering only

some of the electromagnets, providing a differential force that should be able to align the CubeSats, reducing almost to zero pitch and yaw values. While testing, it became clear that in the farthest range of action of the electromagnets, the attracting force is not enough to control the orientation, especially if some of the electromagnets are switched off, while for the close distance trying to orientate them could cause the crashing of the mockups. For this reason and the lack of reliable feedback, the idea of controlling the orientation was not realized.

8 Testing Environment

The project was finalized with the tests required to determine whether the mockups were able to perform docking and undocking operations. Thus, several testing workbenches were proposed to try to simulate optimal conditions to obtain significant results. Although it is not possible to recreate the space environment in the laboratory, meaningful tests can be conducted to find preliminary results about the feasibility of using electromagnets for this purpose.

8.1 Testing Conditions

Conduction of tests required considering several factors while setting the test environment. Firstly, there is the effect of gravity: the satellites in orbit experience free fall but on Earth gravity accelerates them. Secondly, there is air: in orbit, there is almost no air, but in the laboratory, we have to deal with it and possible air disturbances. Another problem was the testing time, which was limited to not more than half an hour at a time due to the rapid discharge of the batteries, and the overheating of the electromagnets. Both issues prevented a continuous and regular testing routine.

Taking into account these effects, the tests were conducted.

8.2 Test Platforms

Three different testing platforms were proposed:

- Hanging the satellites from the ceiling.
- Hanging the satellites from sliders.
- Mounting the satellites in frictionless vehicles.

8.2.1 Hanging the satellites from the ceiling

One proposed workbench was hanging the satellites from the ceiling, as can be seen in Figure 12. With this setup, we wanted to give the mockups the freedom to move in a plane and rotate in the hanging axis. This configuration was the less restrictive and the one that we assumed would be more realistic. However, the tension of the ropes due to gravity created some undesired movements that complicated the testing. Moreover, the fact that the satellites were hanging from a fixed point, and the distance to the ground was not large enough, made the height of the satellites vary slightly. This variation was significant enough to output bad results.

8.2.2 Hanging the satellites from sliders

Another proposed test workbench was to hang the satellites from linear sliders. This way the satellites can have the freedom to move along a line, and to rotate around the hanging axis by adding a thrust bearing. Thus, an aluminum structure was built to mount the linear slider. Although this approach should be very helpful to define the operating thresholds, we found out that the friction in the linear sliders was



Figure 12: hanging-from-the-ceiling test platform

bigger than expected. This implied that the static friction complicated the definition of the minimum distance, and some jerk-off appeared in the linear displacements.



Figure 13: Sliders-based hanging test platform

8.2.3 Mounting the satellites in friction-less vehicles

The last test workbench implied mounting the satellites in almost frictionless vehicles and letting them move freely in a plane. The frictionless condition is achieved by introducing pressurized air into air bearings at the end support of the vehicle. Thus, this configuration should be useful for defining the minimum angle and distance of actuation. Although we encountered some minor issues, such as the forces induced by the air pipes of the vehicles and the tilt of the test bed, this testing method turned out to be the most suitable for this project. To minimize the issues, the team built two rails and put the vehicles between them. This way the freedom of the satellites was reduced, but allowed to have meaningful results. In Figure 14 the testing setup can be seen.

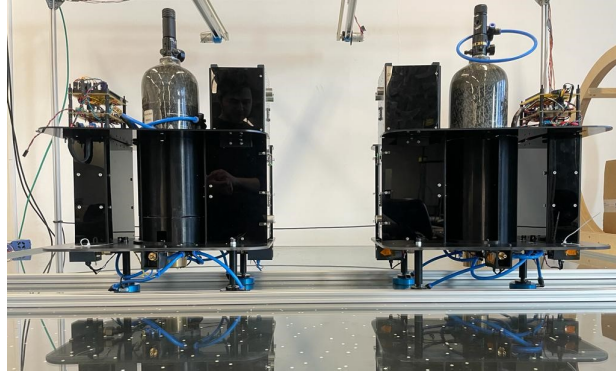


Figure 14: Air bearing testing platform

8.3 Conducting the tests

To analyze the different tasks, several tests were conducted. Mainly the tests were performed by mounting the satellites in the frictionless vehicles, but some of them have been double-checked with the other workbenches. In this section, the detailed procedure of each test will be described. The results of the tests are displayed in Section 9.

8.3.1 Study of the maximum distance for operations

The main objective of the project was to analyze the maximum distance between the two satellites from which attraction is still possible. This result can impact the whole project, maybe even discard it if this distance turned out to be too small.

The steps followed to conduct the tests are given below:

1. Mount the mockups in the vehicles.
2. Find a stable position for one of the vehicles in the frictionless environment and align and fix the other at a certain distance by closing the pressurized air.
3. Send full power to the electromagnets in both vehicles.
4. Repeat until the maximum separation distance is found.

The distance was measured by the lidars and read from the ground station, as well as double-checked with measuring tape on the table to confirm it.

8.3.2 Study of the maximum angle for operations

The philosophy of this test is analogous to the previous one, as it consists of fixing one vehicle and trying several angles between the mockups until finding the maximum angle that can be corrected giving full power to the electromagnets. However, this angle depends on the distance, so the tests were conducted starting from different initial distances. The most suited environment for this type of test is the one in Section 8.2.2 because it allows keeping the satellites in a fixed position, allowing only one degree of freedom, the rotation around the hanging axis. This setup was used to test the maximum distance at which the strength of the electromagnets at maximum

PWM is capable of realigning the satellites. In order to do that, one mockup has been fixed in its position and orientation, while the other was moved.

As the disposition of the polarities of the electromagnets might affect the results, the previous tests were conducted again with different electromagnet configurations. This is done entirely by software by properly defining the different PWM values for each electromagnet.

8.3.3 Study of the capability of Undocking

The objective of this test is to determine if the satellites would be able to perform the undocking maneuver. Theoretically, the undock operation should be achieved by having the same polarity of the electromagnets in both mockups. This test was performed on the air-bearing workbench, with the 3U CubeSat initially docked. Then, the electromagnets of both mockups were assigned the same polarity, creating repulsion forces at the four corners of the mockups.

8.3.4 Study of the interaction with Earth's magnetic field

This test is designed to find out if the natural magnetic field of the Earth interacts with the one generated in the CubeSats with the electromagnets and has some noticeable effects on its dynamics. It was proposed to hang one of the mockups from the ceiling in order to have the most degrees of freedom possible. To conduct this test, the docking face of the satellite is aligned with the North pole of the Earth's magnetic field, and all the electromagnets are configured to have polarity *North*. With this configuration, when the electromagnets are active it is possible to detect if there exists an interaction between them and Earth's magnetic field. The mockup is expected to try to align the docking face with the South pole of the Earth's magnetic field by rotating 180 °at maximum.

8.3.5 Study of the maximum temperature of the mockups

The objective of this test was to analyze the temperatures achieved in the mockups due to the operation of the electromagnets. To conduct this test, the electromagnets were fully powered until the batteries were discharged, which is indicated by the loss of magnetic force. An infrared thermometer was used to measure the temperature of the electromagnets, the surface of the docking side, and the core of the electromagnets. However, these test results are affected by the ambient temperature.

8.3.6 Distance control tests

The next step in the testing phase has been checking the effectiveness of the control algorithm in being able to perform soft docking. It included a continuous trial and error to adjust the various parameters and the necessary checks. The main issue with the controller has been to find a compromise between providing enough PWM to the electromagnets to attract them without risking the high acceleration at a closer distance. The aforementioned problems with the sensors' values did not help with the task, often distorting the real relative distance, thus causing an attractive force much higher than necessary. For this reason, even efforts to try to repel the

satellites applying an opposite polarity did not always have a successful outcome, because the moment gained by the bodies due to the previous attraction was too elevated and the response too delayed. The design that included only ToF sensors only on one side of the CubeSat did not help in that sense.

8.3.7 Velocity control tests

The last tests conducted were about the controller based on the velocity. These tests were conducted to tune the controller values to achieve smooth docking, in accordance with the control scheme, shown in Figure 11. The mockups were stationed at different distances and then their behavior was analyzed. Considering their behavior and their response time, gain values were selected to meet the requirements. As there were four PID controllers, this test was done at multiple distances to see the controller's output and the satellites' overall reaction to that. By doing that, the project was able to achieve relatively smooth docking in the given conditions. However, these tuned parameters cannot be generalized for all the conditions due to the empirical modeling of the system and its realization.

9 Results

In the following section, we will present the results of our research in detail, including an analysis of our data and a discussion of the implications of our findings. Note that these results have to be interpreted as a preliminary conclusion, and they are not accurate enough to infer a decision on whether this project would work in space.

As discussed in Section 8.2.3, the best testing workbench was the one that involved mounting the satellites in frictionless vehicles, which means that all the conclusions have been discovered using this technique, and in some cases even validated with the other workbenches.

9.1 Test Results on Multiple Platforms

A thorough and careful investigation of the mockup docking and reorientation capability was tested by using the three test platforms as defined in section 8. By using the air-bearing platform, docking capabilities were quantified as the function of the relative distance between both satellites. In this series of investigations, both mockups were subjected to different relative distances and were given predefined PWM signals. By altering the distance and PWM signals, it was found that the satellites were able to dock when the relative distance between both was 200mm . After that, control algorithms were designed by using the experimental data which were able to provide smooth docking maneuvers at this distance.

In the second testing platform, namely the sliders-based hanging platform, both satellites were tested for their reorientation capabilities. In this series of tests, both mockups were subjected to different orientation angles relative to each other, conducted at different relative distances. Through these tests, it was found that the electromagnetic field strength had the capability to reorient the satellites and this maximum turn rate was varying as a function of the distance. From these tests, it was deduced that both mockups are able successfully to correct their orientation by the maximum angle of 45° at the distance of 110mm . As the distance decreases, a more range of reorientation was obtained; and when the distance is over 115mm , it has been detected that the magnetic force is not strong enough to overcome the static friction of the workbench.

In the third test, where both mockups were hung by the ceiling, the docking strength of the satellites was checked. It should be noted that in such a testing environment, tests were conducted on the significant influence of gravitational acceleration. Hence, the motivation behind conducting this test was to quantify how the docking mechanism acts under large disturbance forces. During the test, different distance set-points were chosen for analysis. In doing so, it was found that satellites could show docking capabilities even in such conditions. However, the range of docking was halved of what was seen in the air-bearing platform. Nevertheless, it was shown that the combined magnetic field strength of mockups was large enough to counter those disturbances and perform a successful docking maneuver. The results of these tests are summarized in Table 3.

Testing Platform	Initial Distance	Max. Yaw Angle
Hanging from sliders	50mm	80°
Hanging from sliders	75mm	70°
Hanging from sliders	100mm	70°
Hanging from sliders	110mm	45°
Hanging from sliders	115mm	~0°
Hanging from ceiling	100mm	~45°
Air-bearing	200mm	~ 0°

Table 3: Orientation capability of the mockups in the different testing platforms

9.2 Physical Constraints

In light of the outcome of the tests, the physical constraints were defined, i.e., the limits of the workspace where the mockups achieved the docking and undocking operations without external action. In other words, it is the definition of the maximum distance and the maximum angle between the two mockups that still made possible the maneuvers. These findings allowed us to infer other results.

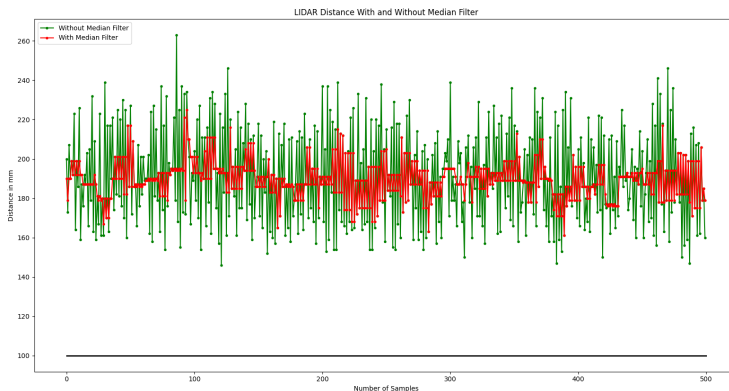
9.2.1 Effect of different structure surface on controller

After studying the limits of the workspace, the team focused on finding a good controller for the maneuvers. At the very beginning of this process, another conclusion was revealed: the material of the docking surface is critical in order to achieve good control. It was discovered that using the chosen Lidars and the Plexiglas as docking surfaces, the distances read by the Lidars were very different from the real ones, and even with calibration they were not precise enough. Thus, different materials were tested as reflectors to find one that would output accurate values. We discovered that Aluminum Panel(99.5%, 2mm) was a better option: it allowed us to measure precisely the distances (passing from an error of $\pm 70\text{mm}$ to $\pm 5\text{mm}$ at a distance of 100mm) and could reduce the thickness of the docking side while giving more strength to the structure. Moreover, it helps the dissipation of the heat created by the electromagnets. The results of this test are plotted in Figure 15.

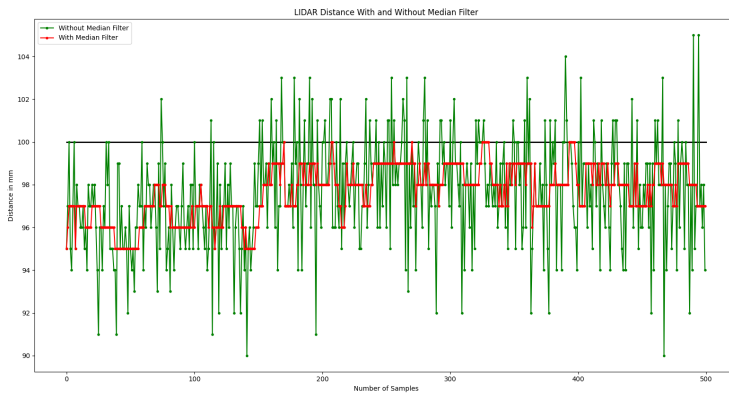
9.2.2 Polarity of the electromagnets

The team decided to study the effect of the polarity of the electromagnets in different situations, trying to find if there is a better configuration. For alignment and docking, all the possible combinations were tested. The configurations are shown in Figure 16.

- Case 1: As expected, this disposition of the polarities is the one that generates the strongest magnetic field. This is caused by the fact that in this situation all the magnets try to attract the ones from the other, independently from the alignment. Thus, this configuration is the one that allowed us to define the limits of the workspace, which is about 200mm in the air bearing testing platform and with a perfect alignment. The main drawback of this configuration is that the strong magnetic field could cause interference with the onboard electronics of the real satellite. But, because this resulted to be the best-reacting



(a) With plexiglass



(b) With aluminium panel

Figure 15: Unfiltered and Filtered Readings of Distances From Lidar

configuration to the various tests, it is believed to be the most indicated for the mission. In addition, as long as it is tested, there is no certainty of a real risk to the hardware.

- Case 2: With this configuration, the team expected a magnetic field similar to the one in Case 1 to be generated. In reality, the experiments showed that this is not true, as the maximum distance was significantly reduced with respect to the previous case (from 200mm to 100mm). It is believed that this is caused by misalignment: the fact that the mockups are not perfectly aligned would mean that some electromagnets are trying to repel each other and the overall attraction force gets compromised.
- Case 3: This case was proposed to correct yaw misalignment. This configuration is believed to be useful when the yaw angle between the two satellites is relatively big as it allows to attract or repel generating a moment, that could be controlled to align the mockups. The problem with this configuration is that, while performing the undocking maneuver, which means inverting the

polarity, the mockups are immediately re-attracted to each other due to the couple of electromagnets on top and on the bottom having opposite polarity.

- Case 4: In opposition to Case 3, this configuration could correct pitch misalignment. As we do not have a good workbench for testing this situation, we can not extract conclusions about it. It might appear that this would generate a similar response as in Case 3 in a different axis but it has to be taken with caution, as the distance between electromagnets 1 and 2 (and 3 and 4) is not the same as the distance between 1 and 4 (and 3 and 2), and the center of mass is not in the middle of the satellite. This means there is no symmetry with respect to Case 3 and has to be studied independently.

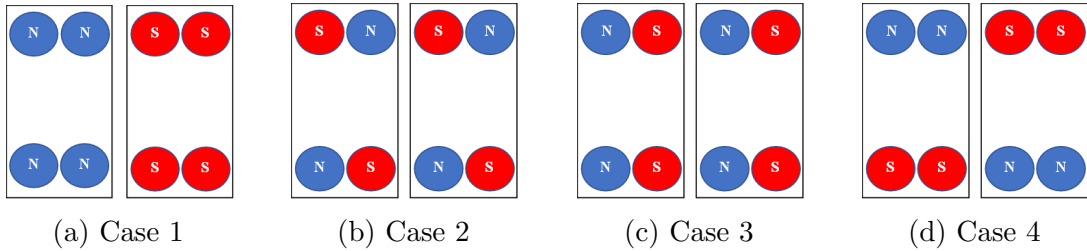


Figure 16: The different configurations of the electromagnets' polarity

9.2.3 Heat generation

Another physical constraint is related to the fact that the electromagnets dissipate heat when they are operating. We noticed that the front panel of the mockups was warm after working with the electromagnets, so we decided to study the maximum temperature achieved by conducting the test described in Section 8.3.5. The results of this test are presented in Table 4. As we can see, the front panel of the mockup is always at 25 °C, but the core of the electromagnets can reach 55 °C. We assume this is the maximum temperature that can be achieved in the cores, as after 15 minutes of operation the CubeSats run out of battery as discussed later in Section 9.5. Note that these results were obtained in the laboratory with an ambient temperature of approximately 21 °C, and are not significant for outer space, but they might be useful as a starting point for future studies.

Time	Front panel Temperature	Core Temperature
5 min	25 °C	35 °C
10 min	25 °C	50 °C
15 min	25 °C	55 °C

Table 4: Temperature of the Mockups at different times

9.3 Undocking

With the results extracted from Section 9.2.2, it was clear that in order to perform undocking the best solution was to use Case 1. At first, the undocking test was

performed giving maximum PWM to the electromagnets with a successful result, and we concluded that it is possible to perform this maneuver. Moreover, the team realized that giving full PWM in the undocking maneuver induced a force that pushed the mockups further than the docking range. This is a good characteristic as it indicates it is possible to generate a wide range of repulsion forces, which are crucial in the development of a precise controller.

9.4 Interaction with Earth's magnetic field

The test described in Section 8.3.4 was conducted and the results will now be discussed. This test was conducted with different power in the electromagnets, and the results are presented in Table 5. As can be seen, the main conclusion is that there exists an interaction between the Earth's magnetic field and the one generated by the electromagnets.

PWM (%)	Rotation (°)
50	25
100	40

Table 5: Rotation of the mockups due to Earth's magnetic field

9.5 Power Constraints

Another important conclusion is related to the power consumption of the satellites. As could be predicted, the maneuvers of alignment, docking, and undocking consume a lot of power. Specifically, when the worst conditions are encountered, the motor drivers need to deliver full power (2A) to the electromagnets until the controller detects a more favorable situation and the PWM can be reduced. We detected a very quick discharge of the batteries in two specific situations: full-throttle conditions and abrupt change in the polarity of the electromagnets. However, we managed to minimize the power-consuming effects of the second situation by deactivating automatically via software the electromagnets before changing the polarity. Nonetheless, the discharge of the batteries was a limiting factor for conducting the tests. When giving full power to the electromagnets, they lasted around 15 minutes. Moreover, we had to stop every 30 minutes to charge them, as the electromagnetic force was significantly decreased. Manifestly, we wanted to test the least favorable situations that require the most power, but this might become an issue and definitely has to be studied more in detail for the real satellites.

9.6 Control Constraints

Controlling the magnetic field strength as the function of velocity and distance is a highly non-linear system, where most of the conventional control methods do not give wanted results. Simulating a mathematical model for such a system requires a lot of computational effort and that resulted in developing an empirical model. To achieve this, a number of tests are required to achieve optimal control. In addition,

due to the non-linear behavior of the system, a fine tuning of the parameters was required that take into account the velocity and position from lidars, and to reach that, the satellite was constrained to always have fine pointing.

10 Recommendations and Future Work

In this Section, the principal suggestions that should be addressed in any continuation of this project and that the team could not handle for reasons of time or other impediments are described.

As already mentioned in the previous sections, the testing phase has been problematic for many causes, and it has been a limiting factor that has barred the project's progression. None of the testing platforms was well-suited for testing in conditions that can be considered representative of the space environment. In particular, it is recommended for future work to fix the air-bearing platform, which was tilted, and the vehicles used to test. Once this is done it should be possible to implement better control approaches such as Fuzzy PID control. To increase the control-space degrees, it is recommended to use additional actuators alongside the electromagnets such as reaction wheels to correct the pose. In addition, the realization of this concept on actual satellites requires a thorough analysis of the impact of electromagnetic fields on the subsystems, and any disturbance forces arising due to this generated field.

Another recommendation has to do with the design of electromagnet casing. The design constraint limited the thickness of the casing to only 1.5mm. As the casing was 3D printed using PLA, the thickness was not enough to hold the cores in place so while initial testing with full PWM, due to the strong force of attraction, the core slipped from the coils and bent the casing. This issue can be fixed by increasing the thickness of the casing to at least 3mm or by machining an aluminum casing.

11 Conclusion

To conclude this project, we will summarize the key findings of our research and discuss their implications for the field. With multiple tests on different testing platforms, it is concluded that electromagnets can be a suitable choice for controlled docking and undocking. However, the tests performed with the current test setups limited the distance of docking range to $200mm$ maximum. With respect to the alignment capabilities, it was found that it is possible to align the satellites starting from an initial angle of 45° and a distance of $110mm$; and even a maximum angle of 80° from a distance of $50mm$.

The effect of different materials on the front panel was also studied, which concludes that aluminum panels (99.5%) are suitable for accurate measurements from the Lidars, and different configurations of the polarity of the electromagnets were tested. However, the docking range could be improved with better test configurations or better test setups. Of the currently available test setups, the most suitable was the air-bearing setup. However, it had some limitations which includes the air-bearing bed not being equally balanced such that the structure does not stay still. On the other hand, the test that involved hanging the satellites from the ceiling proved that it is possible to achieve the objectives in presence of large disturbance forces. Moreover, it was useful to conclude that the Earth's magnetic field has some effect on the orientation of the mockups when the electromagnets were active.

Finally, power and control constraints were analyzed. The power was a restrictive factor while testing, as after about 30 minutes the batteries were already discharged and it should be properly studied in the future. With respect to the control, we managed to develop a simple controller to recognize different situations and actuate accordingly. However, this was useful to demonstrate that the satellites can be controlled and should be a starting point for an accurate controller.

References

- [1] *Discovery kit with STM32F407VG MCU*. UM1472. Revision 7. STMicroelectronics. 2020. URL: <https://www.st.com/resource/en/datasheet/stm32f4discovery.pdf>.
- [2] Sergio Montenegro and Frank Dannemann. “RODOS - real time kernel design for dependability”. In: *DASIA 2009 - Data Systems in Aerospace* (2009).
- [3] *PWM type single channel H-Bridge DC brushed motor driver*. TB9051FTG. Ver.1.1. Toshiba Electronics. 2019. URL: https://www.pololu.com/file/0J1663/TB9051FTG_datasheet_en_20190206.pdf.
- [4] *Raspberry Pi Zero 2 W*. Zero 2 W. Raspberry Pi Foundation. 2021. URL: <https://datasheets.raspberrypi.com/rpizero2/raspberry-pi-zero-2-w-product-brief.pdf>.
- [5] *Time-of-Flight high accuracy proximity sensor*. VL53L4CD. Version 6. STMicroelectronics. 2022. URL: <https://www.st.com/resource/en/datasheet/vl53l4cd.pdf>.